



DEVELOPMENT OF A SEISMIC VULNERABILITY MODEL FOR INDUSTRIAL STEEL BUILDINGS LOCATED IN EUROPE

P. García de Quevedo⁽¹⁾, JM. Castro⁽²⁾, X. Romão⁽³⁾, N. Pereira⁽⁴⁾

⁽¹⁾ *Researcher, Faculty of engineering University of Porto, pablogqi@gmail.com*

⁽²⁾ *Professor, Faculty of engineering University of Porto, jmcastro@fe.up.pt*

⁽³⁾ *Professor, Faculty of engineering University of Porto, xnr@fe.up.pt*

⁽⁴⁾ *PhD, Faculty of engineering University of Porto, nmisp.feup@gmail.com*

Abstract

This paper describes the development of a seismic vulnerability model for industrial portal frame steel buildings located in Europe. The design of this type of buildings is generally governed by wind and snow loads. The derivation of vulnerability the functions for different design classes takes into account different combinations of wind speeds and snow loads. Building-to-building variability is accounted for through the consideration of different sets of synthetic buildings within each class. Each synthetic structure has different geometrical parameters that are consistent with various statistical surveys of the industrial building stock in Europe. The vulnerability assessment is performed through the conduction of response-history analyses in OpenSees on full three-dimensional models of the synthetic portal frame buildings using a set of records consistent with the European seismogenic sources, with different levels of average spectral acceleration. Nonlinear behavior, strength degradation and buckling are considered within the elements of the numerical model. The vulnerability functions are obtained based on a cloud regression performed on the losses, taking into account structural, non-structural elements and contents related to the industrial activity.

Keywords: Vulnerability; Industrial; Steel; Framework; Earthquake



1. Introduction

Earthquake risk assessment on a portfolio scale requires well characterized and defined vulnerability functions for all building classes. Industrial buildings can be critical assets on a portfolio and can be the source of losses due to damage on the structure itself, the machinery or contents within, its nonstructural components, as well as potential disruptions on their activities which can increase the costs caused by the event even further. Typical design practice for these buildings on several European countries does not consider the earthquake loads, as these structures are not usually tall or heavy and may not be particularly susceptible to this kind of actions, and it is in turn governed by wind actions as well as snow and gravity loads. Regardless, even if it is not the most critical factor on these structures' performance, earthquake damage and losses were observed on earthquake events such as L'Aquila (2009), Tohoku (2011), Christchurch (2011) and Emilia Romagna (2012) and should therefore be evaluated. Limited research has been carried out assessing the seismic vulnerability of industrial buildings at a large scale. [1] Suzuki et al (2019) most recently presents fragility curves for Italian code-conforming industrial steel buildings, through nonlinear analyses on equivalent single degree of freedom (ESDOF) systems for different hazard levels. This work is based on the work by [2] Scozzese (2019), who models, for different Italian sites, four different geometrical configurations using ESDOF systems derived from full three-dimensional models, considering both structural and nonstructural elements. These works conclude that collapse is only achieved on high hazard zones for the tested configurations, and that indeed earthquake damage. Similar conclusions regarding the strong performance of these buildings under earthquake actions can be found in [3] Formisiano et al (2016), who constructed vulnerability functions for industrial buildings, considering several different configurations according to information existing buildings and performing two-dimensional analyses. Other studies such as [4] Petruzzelli et al (2012) focus on obtaining the failure probabilities of a group of specific existing buildings and their seismic assessment using 2D and 3D models. All these works assess seismic vulnerability or fragility for industrial steel buildings, but they all focus on smaller regions or specific countries, and there are no works that consider the issue at a continental scale.

This work proposes an innovative framework that will allow to derive analytical seismic vulnerability curves for European industrial buildings, that will have built in uncertainty sources, such as building to building and record to record variability. The basis of this work consist on the construction of a response database, which contains various engineering demand parameters (EDPs) measured on an extensive set of stochastic industrial structures, based on statistical information regarding these kind of structures in Europe [5] (Braconi et al, 2013), for a comprehensive set of records from all European seismogenic sources and at increasing levels of intensity. One of the main advantages of this framework is that due to the creation of the database, it can adapt to a great variety of hazard definitions, locations, design parameters, damage descriptions or consequence models (both economic or time dependent). The vulnerability functions produced with this framework should be compatible with the SERA project (The Seismology and Earthquake Engineering Research Infrastructure Alliance for Europe), which aims to create a full and comprehensive framework for seismic risk modelling at a continental scale.

The following sections will describe the generation of the database, through the creation of stochastic models with varying geometric properties and loads, the numerical modeling, and seismic analysis; as well as the loss computations. Here it will also be described how to implement the framework, with a case study for a selected site in Turkey, through hazard analysis information and using the consequence model proposed in [6] HAZUS – MH MR5 (FEMA-2010).

2. Vulnerability framework

2.1 Building generation

The structures on which this framework focuses are steel portal frame buildings; normally these kind of structures consist on a series of moment resisting frames MRF (made of columns and girders, reinforced on their links), connected perpendicularly by truss elements which are reinforced by braces, creating a concentrically braced frame CBF. The roof is supported by purlins and is strengthened by braces on the extreme bays that help distribute lateral loads.



To generate vulnerability functions consistent with the full European building stock, and correctly account for the uncertainty between structures, it was necessary to consider a considerable sample of buildings, that would encompass a wide array of designs, with different design loads and geometric properties. For this, 12 different classes with 100 different stochastic buildings within them were defined, for a total of 1200 different structures. The main properties that outline the different building classes are wind speeds and snow loads, since these properties are related to the location of the asset, which is something that is normally available on the exposure models, while other properties, like geometric dimensions, materials and other more refined structural properties are not regularly available for this kinds of large scale assessments. The loads for each class were assigned according to Precasteel values [5], discriminating between low, medium and high wind speeds (W1, W2 and W3, respectively), and four levels of snow loading (S1, S2, S3 and S4), shown on Table 1. The wind speeds and snow loads are assigned to each structure within a class by sampling values according to the respective speed or load distribution. For the lower levels of wind and snow loading (W1, W2 and S1, S2 and S3), the distribution was considered to be a uniform distribution. For the stronger classes' values (W3 and S4) a triangular distribution was used for sampling the loads, setting the ultimate values as 35 m/s and 5.0 kN/m² for wind speed and snow load respectively, as they happen to be the maximum values found on the design codes.

Table 1 Wind and Snow classes

Wind Speed [m/s]		Snow Load [kN/m ²]	
W1	$W < 25$	S1	$S < 0.6$
W2	$25 \leq W \leq 29$	S2	$0.6 \leq S < 1.2$
W3	$W > 29$	S3	$1.2 \leq S \leq 2.0$
		S4	$S > 2.0$

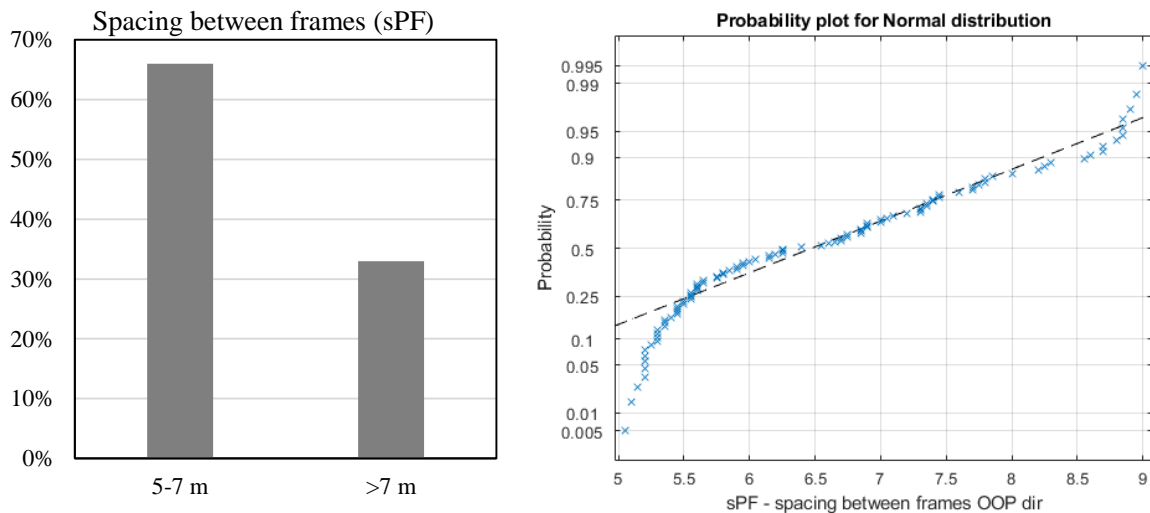


Fig. 1 - Sampling of out-of-plane frame spacing (sPF)

Each building's geometrical properties were taken from sampling the distributions available on the Precasteel report using latin hypercube sampling for each parameter (Figure 1). Figure 2 shows the main geometric properties for each building that were sampled, according to the statistical information where: the in-plan span length (2L), number and spacing of frames in the out of plane (nPF and sPF respectively), the column height (hc), girder slope (θ_g) and whether the base plates were fixed or pinned. Base plate connections vary between fixed, pinned and combinations of both. Information on this regard is limited as these properties cannot be easily extracted on portfolio-based assessment given that they are not beneath the ground and cannot be confirmed through regular surveys.

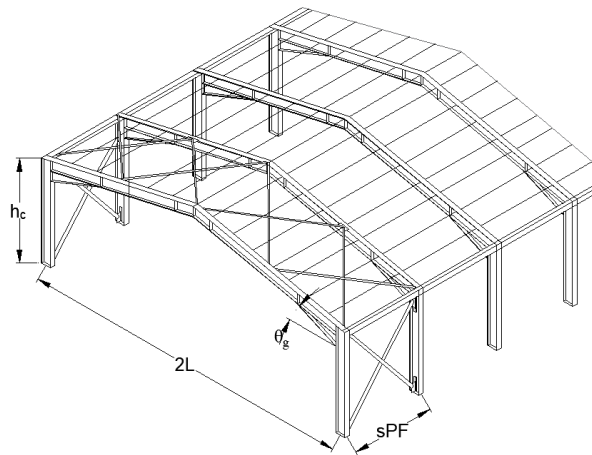


Fig. 2 - Geometric parameters

2.2 Design and steel sections

As previously stated, in many countries across Europe, these kind of structures are not designed considering seismic actions, instead the lateral resisting system is designed to resist the wind loads, and the gravity design considers imposed and snow loads. To be consistent with this, the structural design was carried on following [7] Eurocode 1 (EC1, CEN, 2002) provisions for combinations of gravity, snow and wind loads. Wind actions are computed as following the regulations stated in EN-1991-1-4, which consider the wind speed along with the building's lateral dimensions and roof slope.

Regarding the structural and nonstructural elements, the columns and girders were assumed to be IPE steel profiles, designed according to [8] Eurocode 3 EN 1993-1-1 (CEN, 2005) to resist axial loads, bending with out of plane buckling and the interaction of bending and axial loads, considering the lateral restraint provided by the purlins on girders. CHS profiles were used for the braces (both roof and lateral), and were calculated according to EN 1993-1-1 for tension and buckling on compression, the sections were limited to comply with the slenderness limits proposed by Eurocode 3 for class 1,2 and 3 sections. Base plates were designed following Eurocode 3 component method, which accounts for compression on the concrete and steel elements, and the moment resistance with tension for the bolts and base plate. The purlins' design accounted for gravity loads according to their tributary area, using cold formed steel Z sections. Finally, the nonstructural cladding and roofing elements were considered for all structures as a sandwich panel with dimensions of 1000 x 2500 x 1 mm made of 0.6 mm steel sheets with stiffening ribs and an insulating polyurethane core. The panels were assumed to be of this kind as they are the majority (47% and 33% among all other kinds for lateral and roof cladding, respectively) according to the Precastel report.

2.3 Numerical Modelling

Full three-dimensional models were developed using the open source software [9] OpenSees (PEER,2001), for every of the stochastic buildings within every class, considering all the nonlinear properties for each element in order to capture the possible failure modes these structures can achieve. The modelling assumptions for each element are discussed next.

The braces were modeled to consider the different behaviors these elements exhibit when subjected to earthquake loading, such as yielding in tension, buckling in compression, pinching behavior and fracture. The braces were modeled following the recommendations by [10] Karamanci and Lignos (2014) as a series of force-based fiber elements, with a small imperfection at the center of 0.1% of the effective length, to trigger global buckling, all aggregated with a fatigue material to account for fracture. The model by [11] Hisao et al. (2012) was used for the connections of these elements as well as the gusset plates, which uses a zero length rotational spring with the out of plane gusset plate properties, these elements are then connected by rigid elements, which connect the base plates to the columns and braces as shown in Fig. 3.

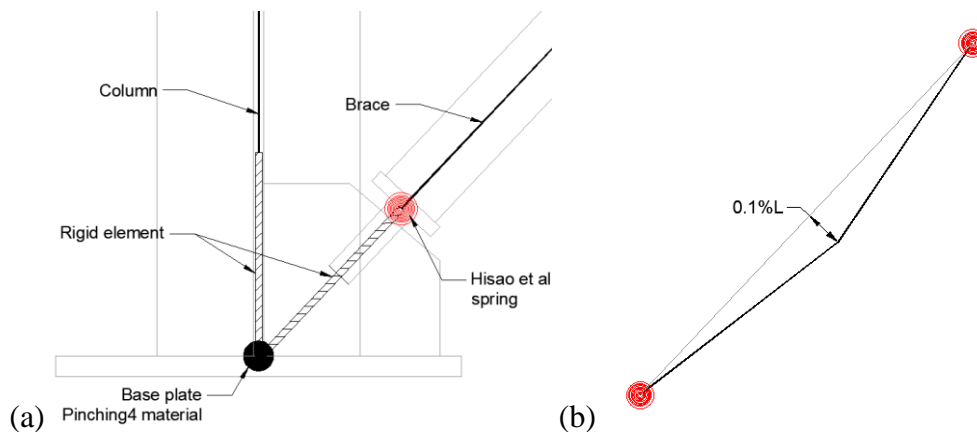


Fig. 3 - Lateral brace modelling (a) connection with column (b) brace modeling according to Karamanci and Lignos

The moment resisting elements, columns and girders, were modelled assuming concentrated plasticity, using [12] Ibarra et al (2005) IMK model springs, which consider strength and stiffness deterioration on steel members, adapted for IPE European commercial profiles following the procedure by [13] Araújo et al. (2015). The sections were considered to be fully laterally restrained. The column and girder connection as well as the apex are reinforced by a haunch, cut from the same steel section as the girder, this region, as well as the apex were modelled as elastic elements, with an increase on the moment of inertia as shown in Fig. 4. The top and bottom of the columns, were modelled as rigid elements, given that at the top the section of the column would be heavily reinforced by the presence of the girder, and the bottom due to the connection with the base plate. Additionally, the columns were modeled as elastic perfectly plastic bilinear springs on their weak direction and pinned bases. At the bottom, the base plates were modelled using a pinching 4 material, calibrated through experimental data [14] (Gomez, 2010), considering different cases regarding the restraint level, as the connections could be considered as fully restrained or pinned for the strong column axis.

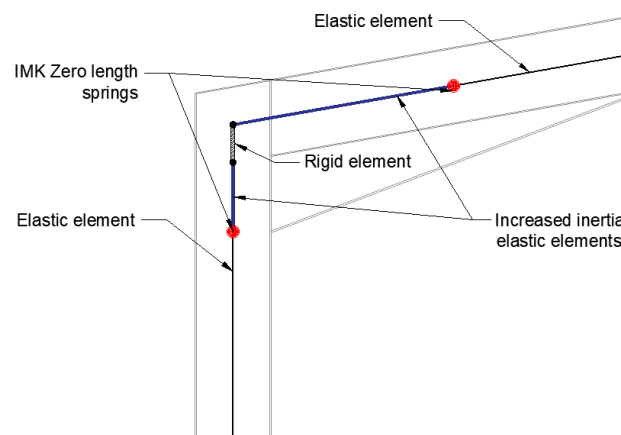


Fig. 4 - Column and girder connection models

The nonstructural cladding elements on the walls and roof were modeled following the approach proposed by [2], in which the series of panels were condensed into a truss system, where a pair of trusses on each bay simulates the behavior of the cladding. Their behavior was simulated using a pinching 4 material, calibrating the results with experimental values (type A tested by [15] De Matteis and Landolfo, 2000). The trusses were modelled on the sides of the building, the roof and one of the facades. The effect of consecutive panels on each bay were accounted following the same hypotheses proposed by [2], where N consecutive panels increase N times the stiffness for each pair of trusses and each row of panels works in series with each other, neglecting the effect of the connections between panels.



2.4 Static analyses

The possible failure modes for the two orthogonal directions were observed through nonlinear static pushover analysis and are displayed for one of the models in Fig. 5. On the X direction analysis, the MRF governs the behavior, and the failure is characterized by a mechanism forming with plastic hinges due to yielding on the base plates and post-peak rotations at the top of the columns and at the edge of the girders (after the haunch), marked on Fig. 5a as circles. The Y direction analysis tested the failure mode of the CBF direction, here, the failure mechanism is caused by buckling on the lateral braces in compression, which can be observed on the deformed shape of Fig. 5c, and yielding on the braces in tension.

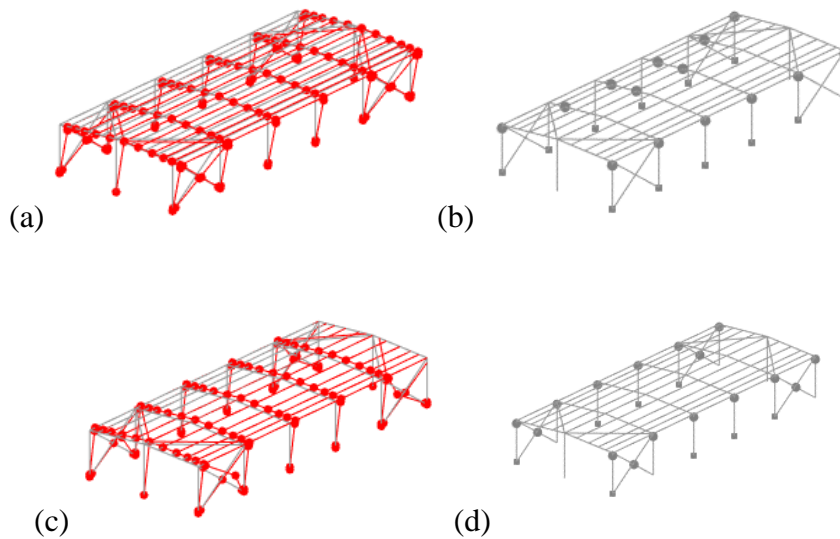


Fig. 5 - Failure modes with (a) deformed shape for pushover on X, (b) plastic hinges for pushover on X, (c) deformed shape for pushover on Y, (d) plastic hinges for pushover on Y

Given the large amount of different stochastic structures, and the complexity of each three dimensional model, performing nonlinear dynamic analysis for each scale factor per ground motion on the set proved to be too computationally and time expensive. Therefore, each structure was simplified into two equivalent single degree of freedom systems (ESDOF), each direction calibrated through nonlinear static analyses, static pushover and cyclic pushover, following the SAC loading protocol. Damping of 2% was assumed for this kind of structures. Fig. 6 shows the calibration for one of the models, using a spring with a pinching behavior for characterizing the cyclic behavior on the braced direction.

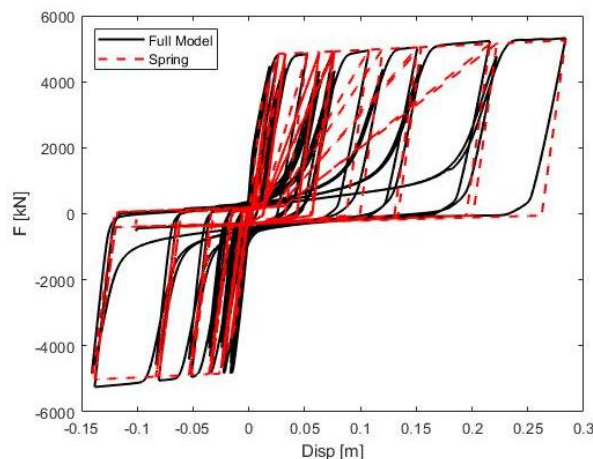


Fig. 6 - ESDOF calibration



2.5 Database

A set of 300 records from the NGA West [16] (Ancheta et al, 2014) and the pan-European engineering strong motion ESM [17] (Luzi et al, 2016) databases was selected, using both horizontal components, with various levels of the geometric mean of the Average Spectral acceleration AvgSa [18] (Kohrangi et al., 2017), using small scale factors. For this framework, average spectral acceleration was adopted as IM to account for the directional effects of being a three dimensional structure as well as the large dispersion found between the fundamental periods for each and every stochastic model, as it ranges from 0.13s to 1.39s on the MRF direction and 0.11 and 0.42 on the CBF direction. It also allows to directly compare vulnerability functions across different building taxonomies. A central period of $T_c=0.75$ s was selected, with a period range of $0.2T_c \leq T_c \leq 1.5 T_c$ or 0.15s to 1.125s.

Nonlinear time history analyses were carried out in OpenSees on all the ESDOF models for all structures, performing incremental dynamic analysis using the hunt, trace and fill algorithm [19] (Vamvatsikos & Cornell, 2004). The outcome of these analysis was condensed into a large database that contains the responses of all 1200 structures to increasing levels of intensity, until collapse, for all the 300 pairs of motions, recording the maximum transient and residual drifts, as well as the maximum accelerations in both horizontal directions. This extensive response database allows for multiple outputs, depending on the post processing and disaggregation of information, since it associates information of each building's geometrical and loading parameters with the building intensity and the responses. With this is possible to disaggregate the information in different ways and create vulnerability functions that work on a continental scale, consistently incorporating the uncertainty.

2.6 Record filtering

To illustrate an application of the framework, the records were filtered using a group of conditional spectra, obtained from hazard analysis on a site located in Atasehir, Istanbul, Turkey, using the hazard information available in the SHARE model [20] (Woessner et al, 2015) for the exceedance probabilities shown in Table 2, with their corresponding return periods and intensities. Sets of 20 records per return period (with their respective scaling factor) were extracted using the conditional mean spectrum record selection algorithm proposed by [21] Baker and Lee (2018), adapted for AvgSa as shown in Fig. 7. Once the records and their scaling factors are known, the building's responses are extracted from the database or interpolated from the IDA curves for cases where the scaling factor is not exactly found for that record in the database.

Table 2 Hazard analysis information

P.o.e. in 50 years	Return period [years]	AvgSa _{0.15:1.125s} [g]
60%	55	0.137
30%	140	0.226
10%	475	0.416
5%	975	0.573
3%	2475	0.819
1%	4975	1.027
0.5%	9950	1.189
0.2%	24975	1.558

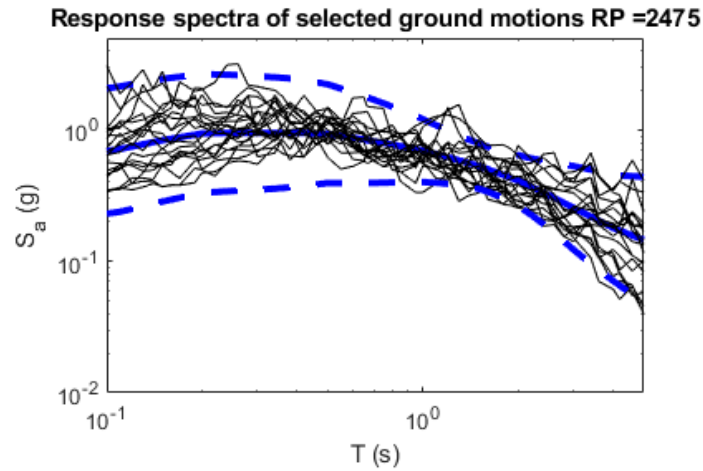


Fig. 7 – Record filtering for return period of 2475 years

2.7 Loss calculations

The next step within the framework is to calculate the losses that correspond to each building at a given intensity, which is why a damage and consequence model is required. Data regarding the consequence values of loss for different damage states on industrial buildings is scarce and not easily obtained, therefore to illustrate the final steps of the framework, the HAZUS - MH MR5 (FEMA, 2010) approach was adopted, which contains different loss values for industrial facilities, taking into account structural, nonstructural drift and acceleration sensitive elements (NSD and NSA, respectively) and contents. Therefore, the different EDPs found from the analyses were converted to losses directly following this approach. Given the nature of this framework, different consequence models can be plugged in according to the required output.

Table 3 Structural and Nonstructural damage state limits. Adapted from HAZUS - MH MR5

Nonstructural Damage States				
Component type	Slight	Moderate	Extensive	Complete
Drift Sensitive (%)	0.004	0.008	0.025	0.05
Acceleration Sensitive [g]	0.30	0.60	1.20	2.40
Structural Damage States Drifts				
Structure type	Slight	Moderate	Extensive	Complete
Steel Moment Frame	0.006	0.012	0.030	0.080
Steel Braced Frame	0.005	0.010	0.030	0.060

HAZUS - MH MR5 defines five discrete damage states for all types of structures and all types of structural and nonstructural elements, Slight, Moderate, Extensive and Complete. Table 3 shows the mean demand values, either drift or acceleration, for which the guidelines assume the structure to be in a given damage state. The variability considered for the different curves across the damage states is obtained from HAZUS - MH MR5, using the set of precomputed variabilities, with values of $\beta_{T,ds}=0.3$ (Structural), $\beta_{T,ds}=0.5$ (NSD) and $\beta_{T,ds}=0.6$ (NSA). These values help define predefined fragility curves as lognormal distribution curves $P(DS|EDP)$, for the different taxonomies, for this case study the curves selected are for steel moment resisting frames and steel braced frames. The losses were computed accounting for transient drifts, maximum acceleration and the probability of demolition given the residual drifts. Structural losses are related to the



maximum drift, while nonstructural losses are divided into drift-sensitive and acceleration-sensitive. The losses due to repairs on the structure are combined using the percentages of table 7.3 on the HAZUS - MH MR5 manual, where acceleration sensitive nonstructural elements on industrial facilities amount to 62% of the total building replacement cost, structural losses 27% and finally drift-sensitive nonstructural elements 11%. To account for permanent drifts, works by [22] Elkadi et al (2019) and [23] Ramirez and Miranda (2012) were considered, accounting for the probability of demolition for a given value of permanent drift. The total loss for a given EDP is computed accounting for demolition and collapse with Eq. 1

$$E[L_T|EDP] = E[L_T|NC \cap R] P(NC \cap R|EDP) + E[L_T|NC \cap D] P(NC \cap D|EDP) + E[L_T|C] P(C|EDP) \quad (1)$$

Where $E[LT|NC \cap R]$ is the expected loss when the structure does not collapse and is repaired, computed as the weighted sum of the losses (structural and nonstructural) obtained by evaluating the corresponding EDP on the curve found by the convolution of the damage states $P(DS|EDP)$, given for this case by the lognormal distributions described by their means found in Table 3 and their respective standard deviation, with the expected loss per damage state $E[LT|DS]$, given by Table 4. $E[LT|NC \cap D]$ is the loss when the structure does not collapse and is demolished, assuming the loss to be 1. The probability of demolition $P(NC \cap D|EDP)$ is described by the lognormal distribution with a median residual drift value of $\mu_{RDR}=0.96\%$ with a standard deviation, $\sigma_{\ln RDR}=0.3$ for European steel buildings according to [22]. Finally, $E[LT|C]$ is the loss associated with the collapse of the building, which also equals a loss ratio of 1.

Table 4 Normalized repair/replacement costs: Adapted from HAZUS - MH MR5 15.2 15.3 15.4

Type	Slight	Moderate	Extensive	Complete
Structural	0.02	0.10	0.50	1.0
Drift-sensitive nonstructural	0.02	0.10	0.50	1.0
Acceleration-sensitive nonstructural	0.02	0.10	0.30	1.0

2.8 Vulnerability curves

Repeating the previous step for all structures, records and return periods results in stripes of loss values for the different levels of AvgSa. The mean and dispersion for each stripe was computed, assuming that the loss at every stripe follows a Weibull or skewed distribution. Fig. 8 shows the vulnerability curve for wind class W1 and snow S1, with the different stripes of loss found at each intensity level. The dispersion in the curves is attributed to mainly three aspects, the building to building variability, the record to record variability and the intra building variability.

The building to building variability happens due to the amount of geometrical combinations existing within the stochastic set, since changing parameters such as the height and span of the structures greatly alters the behavior. The span causes an increase on the girder size, which in turn causes the column's sections to be increased, impacting on the structures' stiffness. Record to record variability depends on the hazard information available, as the records come from different seismogenic sources and will cause different responses to the same intensity. Finally, the intra structure variability is caused by the two perpendicular structural systems present on these kind of buildings, since they have very different responses to seismic excitation. The MRF will always have a larger period, larger drifts, less damage for said drifts, and lower acceleration, controlled by the size of the members and therefore, sensitive to the design load; while the CBF will almost always have much smaller deformations, higher damage to the members for smaller drifts and higher acceleration values. The fact that even for large levels of intensity (max AvgSA), the mean losses are still below 40% and given the relatively low number of collapses achieved during the analyses for this levels of seismic excitation, prove that these structures, while susceptible to earthquake damage,



are not particularly vulnerable to earthquake loading, and the design considerations of prioritizing the effects of wind and snow seem to be adequate as other similar works have concluded

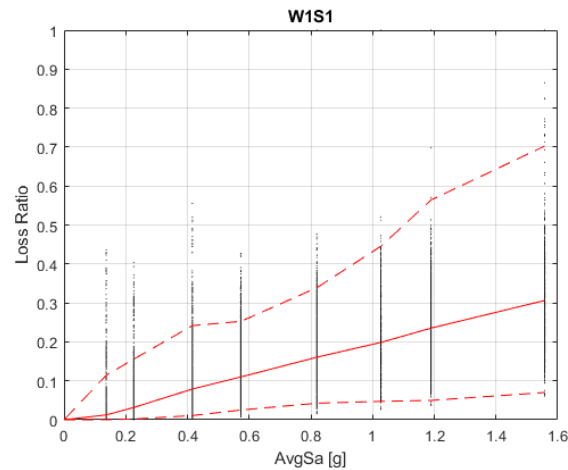


Fig. 8 - Vulnerability curve W1S1

3. Sensitivity analysis

Given the flexibility of the framework and the extensive array of properties available in the database, it is possible to perform more detailed selections within the classes, to reduce the building to building variability in cases where more information regarding the geometry of the building is known. Fig. 9a shows the vulnerability curve for a sub-selection of buildings within class W1S1 which contains only structures with a column height (hc) shorter than 6m, with a portal frame span ($2L$) smaller than 25m, and less than 15 out of plane frames (nPF). This way some of the inter building dispersion can be reduced, and it is possible to create more appropriate or customized functions by creating sub classes, modifying the selection parameters.

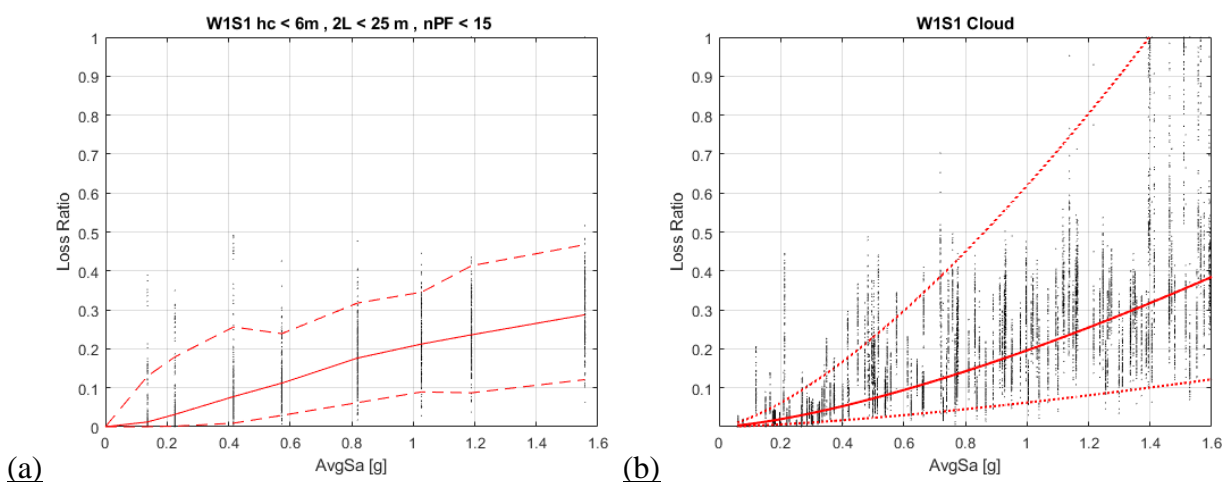


Fig. 9 – (a) Vulnerability curve W1S1, filtering by hc , $2L$ and nPF (b) Vulnerability curve W1S1 all original records through cloud analysis

This framework proposes the use of a target spectrum in order to derive more hazard consistent vulnerability curves. Even if the scope of this work is to derive vulnerability curves useful for anywhere in Europe, the record to record variability that can arise from using records from all European seismogenic sources will lead to very large levels of dispersion as mentioned before. The use of this target spectra reduces significantly the



variability. Alongside the curves found, a cloud analysis with all the records with their original scaling factors was performed for all buildings within a class (W1S1), fitting the results to an exponential regression (or linear regression in log space). The results shown in Fig. 9b illustrate how the dispersion is increased even further, as the record to record variability for all the different seismogenic sources on a continental scale analysis lead to widely different results for the same IM. Therefore, it is encouraged that some hazard information is used in tandem with this framework to improve the final results.

4. Conclusions

The framework presented on this work allows for the creation of vulnerability curves that will be valid for industrial buildings across different territories within Europe. The creation of the response database for the extensive stochastic set of buildings and seismological sources enables the possibility to adapt the framework to different locations with their corresponding hazard level as well as diverse damage definitions, whether they are global or element based, together with consequence models that are consistent with these damage definitions and that provide the corresponding losses. Inspecting the resulting vulnerability curves for the damage and consequence models applied here reinforces the notion that this kind of structures are not particularly vulnerable to earthquake action and even though they sustain some level of damage, it only happens on higher, less frequent, intensities. Additionally, the damage observed in these buildings was primarily due to the acceleration response (which impacts nonstructural elements) and not due to large displacement demands. This observation can also be attributed to the fact that nonstructural elements are normally the costliest components on industrial steel buildings. The dispersion found in the results reflects the uncertainty that exists when characterizing these buildings on a portfolio level and can be optimized through filtering depending on the available information regarding the building's geometry and design characteristics beyond the location-related parameters. The record to record variability also considered in the curves can be in turn controlled with an appropriate hazard analysis for the site of interest when performing risk assessment.

Further improvements that can be added in the future would incorporate elements to the database that were not considered within the stochastic building set, such as including crane loads, truss girders and different cladding materials, adding new building classes and expanding the different ways to group the data.

5. Acknowledgements

The research reported in this paper has been partially developed under the SMARTER project – Seismic Urban Risk Assessment in Iberia and Maghreb (PT-DZ/0002/2015), funded by the Portuguese Foundation for Science and Technology and the SERA project (Seismology and Earthquake Engineering Research Infrastructure Alliance for Europe) funded by the European Union's Horizon 2020 research and innovation programme.

6. References

- [1] Suzuki A, Iervolino I (2019) Seismic Fragility of Code-conforming Italian Buildings Based on SDoF Approximation, *Journal of Earthquake Engineering*, DOI: 10.1080/13632469.2019.1657989
- [2] Scozzese F, Terracciano G, Zona A, Della Corte G, Dall'Asta A, Landolfo R (2018) Modeling and Seismic Response Analysis of Italian Code-Conforming Single-Storey Steel Buildings, *Journal of Earthquake Engineering*, 22:sup2, 2104-2133, DOI: 10.1080/13632469.2018.1528913
- [3] Formisano A, Castaldo C, Iannuzzi I. (2016). Seismic Vulnerability and Fragility of Industrial Steel Buildings Affected by the Emilia-Romagna Earthquake.
- [4] Petruzzelli F, Della Corte G, Iervolino I (2012) Seismic Risk Assessment of an Industrial Steel Building Part 1: Modelling and Analysis. *Procedures of 15WCEE*, Lisboa, Portugal
- [5] Braconi A, Osta A, Dall'Asta A, Leoni G, Möller S, Hoffmeister B, Karamanos S, Varelis G, Alderighi E, Coscetti C, Salvatore W., Gracia J, Bayo E, Mallardo R, Bianco L, Filipuzzi P, Vasilikis D, Tsintzos P, Estanislau S, Hradil P. (2013). Prefabricated steel structures for low-rise buildings in seismic areas (Precastel). 10.2777/5499.



- [6] FEMA (2010) Multi-hazard loss estimation methodology. Earthquake Model. HAZUS – MH MR5 Technical Manual, Federal Emergency Management Agency, Mitigation Division, Washington, D. C., United State
- [7] CEN (2002) NP ENV 1993-1-1 Eurocode 3: design of steel structures – Part 1-1: general rules and rules for buildings, European Committee for Standardization, Brussels, Belgium
- [8] CEN (2005) NP ENV 1993-1-8 Eurocode 3: design of steel structures – Part 1-8: design of joints, European Committee for Standardization, Brussels, Belgium
- [9] PEER (2011) OpenSees: open system for earthquake engineering simulation, Pacific Earthquake Engineering Research Center, University of California, Berkeley, CA. United States.
- [10] Karamanci E, Lignos D. (2014). Computational Approach for Collapse Assessment of Concentrically Braced Frames in Seismic Regions. *Journal of Structural Engineering*. A4014019. 10.1061/(ASCE)ST.1943-541X.0001011.
- [11] Hsiao P, Roeder C. (2012). Improved Analytical Model for Special Concentrically Braced Frames. *Journal of Constructional Steel Research*. 73. 80–94. 10.1016/j.jcsr.2012.01.010.
- [12] Ibarra LF, Medina RA, Krawinkler H (2005) Hysteretic models that incorporate strength and stiffness deterioration, *Earthquake Engineering and Structural Dynamics*, 35, 1489-1511.
- [13] Araújo M, Macedo L, Castro JM (2015) Calibration of strength and stiffness deterioration hysteretic models using optimization algorithms, In Proceedings, *8th International Conference on Behavior of Steel Structures in Seismic Areas STESSA*, Shanghai, China.
- [14] Gomez IR (2010) Behavior and design of column base connections, PhD thesis, University of California, Davis, CA.
- [15] De Matteis, G., Landolfo, R. (2000) Modelling of lightweight sandwich shear diaphragms for dynamic analyses, *Journal of Constructional Steel Research* 53(1), 33–61. doi:10.1016/S0143-974X (99)00038-3.
- [16] Ancheta T, Darragh R, Stewart J, Seyhan, E, Walter S, Chiou B, Wooddell, K, Graves R, Kottke A, Boore D, Kishida T, Donahue J. (2014). NGA-West2 database. *Earthquake Spectra*. 30. 10.1193/070913EQS197M.
- [17] Luzi L, Puglia R, Russo E, ORFEUS WG5 (2016). Engineering Strong Motion Database, version 1.0. Istituto Nazionale di Geofisica e Vulcanologia, Observatories & Research Facilities for European Seismology. doi: 10.13127/ESM
- [18] Kohrangi M., Bazzurro P., Vamvatsikos D., Spillatura A. (2017) Conditional spectrum-based ground motion record selection using average spectral acceleration. *Earthquake Engng Struct. Dyn.*, 46: 1667– 1685. doi: 10.1002/eqe.2876.
- [19] Vamvatsikos, D., & Cornell, C. A. (2004). Applied Incremental Dynamic Analysis. *Earthquake Spectra*, 20(2), 523–553. <https://doi.org/10.1193/1.1737737>
- [20] Woessner J., Danciu L., D. Giardini and the SHARE consortium (2015), The 2013 European Seismic Hazard Model: key components and results, *Bull. Earthq. Eng.*, doi:10.1007/s10518-015-9795-1.
- [21] Baker J. W., Lee C. (2018). An Improved Algorithm for Selecting Ground Motions to Match a Conditional Spectrum. *Journal of Earthquake Engineering*, 22(4), 708–723.
- [22] Elkady A, Güell G, Lignos D G., (2019) Proposed methodology for building-specific earthquake loss assessment including column residual axial shortening. *Earthquake Engng Struct Dyn.* 2019; 1– 17. <https://doi.org/10.1002/eqe.3242>
- [23] Ramirez MC, Miranda E (2012) Significance of residual drifts in building earthquake loss estimation, *Earthquake Engineering and Structural Dynamics*